journal

J. Am. Ceram. Soc., **82** [4] 873–81 (1999)

Ultrafine Barium Titanate Powders via Microemulsion Processing Routes

John Wang,[*,†] Jiye Fang,[†] Ser-Choon Ng,[‡] Leong-Ming Gan,[§,¶] Chwee-Har Chew,[§] Xianbin Wang,[‡] and Zexiang Shen[‡]

Department of Materials Science, Department of Physics, Department of Chemistry, and Institute of Materials Research and Engineering, National University of Singapore, Singapore 119260

Three processing routes have been used to prepare barium titanate powders, namely conventional coprecipitation, single-microemulsion coprecipitation using diether oxalate as the precipitant, and double-microemulsion coprecipitation using oxalic acid as the precipitant. A single-phase perovskite barium titanate was obtained when the double-microemulsion-derived oxalate precursor was calcined for 2 h at a temperature of as low as 550°C, compared to 600°C required by the single-microemulsion-derived precursor. A calcination for 2 h at >700°C was required for the conventionally coprecipitated precursor in order to develop a predominant barium titanate phase. It was, however, impossible to eliminate the residual TiO_2 impurity phase by raising the calcination temperature, up to 1000°C. The microemulsion-derived barium titanate powders also demonstrated much better powder characteristics, such as more refined crystallite and particle sizes and a much lower degree of particle agglomeration, than those of the conventionally coprecipitated powder, although they contained ~0.2 wt% $BaCO_3$ as the impurity phase.

I. Introduction

BARIUM TITANATE ($BaTiO_3$) is among the most important electroceramics for applications in electronics and microelectronics owing to its excellent ferroelectric, piezoelectric, and dielectric properties.[1,2] It is widely used as the main constituent in many types of electroceramic devices such as multilayer capacitors and positive temperature coefficient resistors (PTCR). Solid-state reaction between $BaCO_3$ and TiO_2 in an equimolar ratio at temperatures >1200°C has often been used to prepare $BaTiO_3$ powders.[3] Unfortunately, the conventional solid reaction is associated with many disadvantages including the high impurity and poor powder characteristics, represented by a coarse particle size, wide particle size distribution, irregular particle morphology, and a high degree of particle agglomeration. It is therefore not surprising to note that a large number of chemistry-based novel processing routes have been developed for the production of fine and homogeneous $BaTiO_3$ powders. These include coprecipitation,[4–6] sol–gel processing,[7–9] hydrothermal synthesis,[10,11] reactions in molten salts,[12,13] processing from polymeric precursors,[14,15] and oxalate[16–18] and citrate[19–21] routes, as have been reviewed by Phule and Risbud[1] and Chaput *et al.*[22] Some of these novel processing routes have demonstrated many apparent advantages over the conventional solid reaction in producing a fine and homogeneous $BaTiO_3$ powder, although the degree of success varies considerably from one technique to another.

Several technologically important ceramic systems have recently been synthesized from water-in-oil microemulsions.[23,24] The microemulsion-derived ceramic powders are much finer in particle size, narrower in particle size distribution, and higher in both composition homogeneity and sinterability than those prepared via many other chemistry-based processing routes.[24,25] A water-in-oil microemulsion, which consists of an oil phase, a surfactant, and an aqueous phase, is a thermodynamically stable isotropic dispersion of the aqueous phase in the continuous oil phase.[26] The size of the aqueous droplets is in the range of 5 to 20 nm, rendering the microemulsions optically transparent. A precipitation/coprecipitation reaction will be brought about in the nanosized aqueous domains when droplets containing appropriate reactants collide with each other. Each of these aqueous droplets will be acting as a nanosized reactor for forming nanosized precursor particles.

It is both scientifically interesting and technologically challenging to synthesize an ultrafine, preferably nanosized, barium titanate powder. Microemulsions offer the feasibility of refining the particle sizes to nanometer scale, although they are associated with such disadvantages as a low production yield and high production cost when the oil and surfactant phases are washed off. It is, however, possible to recycle them when the microemulsion processing technique is fully developed and matured for industrial applications. Schlag and co-workers[27] have recently tried without success to synthesize fine barium titanate particles of high purity from an inverse microemulsion consisting of decane (oil phase), a nonionic surfactant (Genapol OX30, Hoechst, Switzerland), and an aqueous phase containing barium and titanium chlorides. Oxalate precipitates were formed in the nanosized microemulsion domains; however, they were unable to obtain a single-phase $BaTiO_3$ when the precursor was calcined at various temperatures ranging from 400° to 1200°C. They attributed the failure to the inhomogeneous dispersion of titanium in microemulsion droplets and the adverse effects of residual surfactant and chlorine counterions left in the precursor. To study the feasibility of deriving ultrafine $BaTiO_3$ powders from microemulsions containing no chlorine ions in the aqueous phase, both single-microemulsion and double-microemulsion processing routes were employed in the present work. In the double-microemulsion processing route, oxalic acid was used as the precipitant. Diethyl oxalate is sparingly soluble in water (aqueous droplets) and slowly releases oxalic acid when decomposed. It was chosen as the precipitant in the single-microemulsion route, in order to avoid a very rapid coprecipitation reaction which may result in the formation of a highly agglomerated and chemically heterogeneous $BaTiO_3$ powder. The microemulsion-derived $BaTiO_3$ powders were characterized in a close comparison with the one derived from conventional coprecipitation of oxalates.

P. P. Phule—contributing editor

Manuscript No. 190743. Received September 2, 1997; approved August 27, 1998.
Supported by Research Grant No. RP960692 from the National University of Singapore.
[*]Member, American Ceramic Society.
[†]Department of Materials Science.
[‡]Department of Physics.
[§]Department of Chemistry.
[¶]Institute of Materials Research and Engineering.

II. Experimental Procedure

(1) Starting Materials

The starting materials used in the present work included barium nitrate (>99.0%, Merk, Germany), titanium(IV) chloride (>99.0%, Hayashi Pure Chemical Industries Ltd., Japan), a high-purity cyclohexane (AJAX Chemicals, Australia), a nonionic surfactant consisting of poly(oxyethylene)$_5$ nonyl phenol ether (NP5) and poly(oxyethylene)$_9$ nonyl phenol ether (NP9) (NP5:NP9 weight ratio: 2:1, Albright and Wilson Asia Pte Ltd, Singapore), oxalic acid dehydrate (>99.9%, J. T. Baker Int., USA), together with an ammonia solution (concentration: 28.0–30.0 wt%, J. T. Baker Inc., USA) and nitric acid (Hetalab Chemical Corp., USA).

(2) Aqueous Solution Containing 0.12M $Ba(NO_3)_2$ + 0.12M $TiO(NO_3)_2$

An aqueous solution of titanium oxynitrate was prepared by following the procedures of Kudaka *et al.*[28] For this, an appropriate amount of deionized water was added slowly to preweighed titanium tetrachloride ($TiCl_4$) which was kept cool (~0°C) and was constantly stirred. A cold ammonia solution (12 wt%) was then added to the aqueous solution, resulting in the formation of titanium hydroxide hydrates. In order to remove the chloride ions, the gelatinous precipitates were filtered and washed repeatedly using deionized water until the pH of the filtrate was close to 7.0 and no trace of chloride was detected by $AgNO_3$. Titanium oxynitrate in aqueous solution was then prepared by dissolving the white precipitates in an appropriate amount of 3.0*M* HNO_3, immediately followed by the concentration determination of Ti^{4+} using ICP (inductively coupled plasma, Thermo Jarrell Ash, IRIS/AP). The concentration of $TiO(NO_3)_2$ in the solution was adjusted to 0.24*M* by adding an appropriate amount of deionized water. To prepare the aqueous solution containing 0.12*M* $Ba(NO_3)_2$ + 0.12*M* $TiO(NO_3)_2$ with an equimolar ratio of Ba^{2+}/Ti^{4+}, an equal volume of 0.24*M* $Ba(NO_3)_2$ solution was combined with the aqueous solution of titanium oxynitrate.

(3) Phase Diagrams

The procedure of establishing a partial phase diagram at room temperature for the ternary system consisting of cyclohexane, NP5 + NP9, and an aqueous solution has been detailed elsewhere.[23,24] To locate the demarcation between the microemulsion and nonmicroemulsion regions, the aqueous phase was titrated into a mixture of given cyclohexane-to-surfactant ratio. Thorough mixing of the three components was achieved using a Vortex mixer. Microemulsion compositions appear optically transparent when the size of aqueous droplets is in the range of 5 to 20 nm, because the nanosized aqueous droplets do not cause a substantial degree of light scattering. A series of such demarcation points were obtained by varying the cyclohexane-to-surfactant ratio. Partial phase diagrams at room temperature for two ternary systems were established. They consisted of cyclohexane, NP5 + NP9, and an aqueous phase containing 0.12*M* $Ba(NO_3)_2$ + 0.12*M* $TiO(NO_3)_2$ and 0.34*M* oxalic acid, respectively.

(4) Preparation of $BaTiO_3$ Powders

As shown in Fig. 1, three processing routes were used to prepare $BaTiO_3$ powders in this work, namely, the conventional coprecipitation reaction (CCR), single-microemulsion coprecipitation (SMC) using diether oxalate as the precipitant, and double-microemulsion coprecipitation (DMC) using oxalic acid as the precipitant.

For the CCR, 200 mL of the aqueous solution containing 0.12*M* $Ba(NO_3)_2$ + 0.12*M* $TiO(NO_3)_2$ was titrated dropwise into 200 mL of 0.38*M* oxalic acid ($H_2C_2O_4$) solution while being vigorously stirred. The resulting coprecipitates were washed repeatedly using deionized water and recovered by centrifugation, followed by vacuum-drying at room temperature for 48 h.

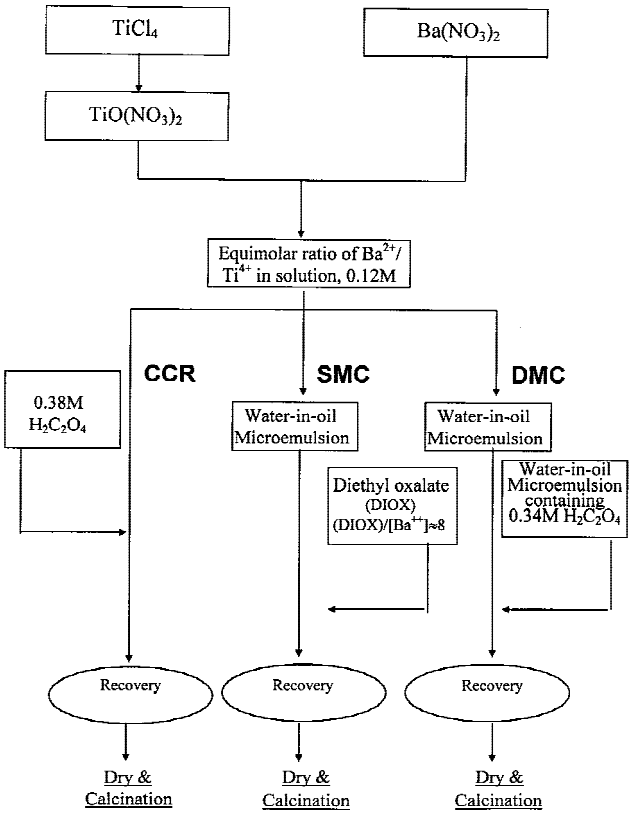

Fig. 1. Flow chart for the preparation of $BaTiO_3$ powders via three processing routes.

In SMC, a microemulsion composition consisting of 64.0 wt% cyclohexane, 16.0 wt% NP5 + NP9, and 20.0 wt% aqueous phase containing 0.12*M* $Ba(NO_3)_2$ + 0.12*M* $TiO(NO_3)_2$ was first prepared. The concentration of $Ba(NO_3)_2$ and $TiO(NO_3)_2$ was ~0.02*M* in the overall microemulsion composition. The coprecipitation was brought about by mixing 780 g of microemulsion composition with 21.7 g of diether oxalate via vigorously stirring the mixture for 24 h. At the same time, the mixture was heated slowly to 40°C. To retrieve the coprecipitates formed in the microemulsion, the oil and surfactant phases were washed off using distilled ethanol and the precursors were then recovered by centrifugation, followed by washing using deionized water and vacuum-drying at room temperature for 48 h.

For DMC, two microemulsion compositions, both consisting of 64.0 wt% cyclohexane, 16.0 wt% NP5 + NP9, and 20.0 wt% aqueous phase, were prepared. The aqueous phases in the two microemulsions were 0.12*M* $Ba(NO_3)_2$ + 0.12*M* $TiO(NO_3)_2$ and 0.34*M* $H_2C_2O_4$ solutions, respectively. Coprecipitation reaction was made to take place when the two microemulsions were mixed together by vigorously stirring the mixture for 3 h at room temperature. The resulting precursor was recovered and dried by following the same procedures as those in the SMC route.

(5) Precursor and Powder Characterizations

The as-dried precursors from the above three processing routes were characterized using thermogravimetric analysis (TGA2950, Du Pont Instruments, Wilmington, DE) and differential thermal analysis (DTA1600, Du Pont Instruments) with alumina as the reference at a heating rate of 10°C/min in air from room temperature up to 950°C. They were then calcined in air at various temperatures, up to 800°C, followed by phase identification performed at room temperature using a (Cu$K\alpha$) X-ray diffractometer (PW1729, Philips, 7602 EA Almelo, The Netherlands) and a Raman scattering spectrometer (Ramascope

2000, Renishaw, UK) with a spectral resolution of 2 cm^{-1} using a near-infrared laser ($\lambda = 782$ nm) as the exciting source. They were also characterized using a FTIR spectrometer (FTS135, BIO-RAD Laboratories, Inc., Cambridge, MA) over the spectrum range 4000–400 cm^{-1} and the spectra were averaged out from 64 scans with a nominal resolution of 2 cm^{-1} (KBr pellet). On the basis of XRD line broadening at half-maximum of the (110, 101) peaks, crystallite sizes in the calcined $BaTiO_3$ powders at various temperatures were estimated using the Scherrer equation.[29] The particle/agglomerate size distribution was measured using a laser scattering particle size analyzer (LA-910, Horiba, Miyanohigashi Kisshoin Minami-Ku, Kyoto, Japan). A gas sorption analyzer (Nova 2000, Quantachrome Corp., Boynton Beach, FL), a transmission electron microscope (100CX, JEOL, Japan) and a scanning electron microscope (JSM-35CF, JEOL, Japan) were employed to analyze the specific surface area and particle/agglomerate morphology of these powders, respectively. The analysis of carbon content was performed on the powders calcined at 800°C using a Perkin-Elmer elemental analyzer (2400 CHN) and the Ba/Ti ratios in these powders were determined using ICP (IRIS/AP, Thermo Jarrell Ash, USA). For this, a small amount of each $BaTiO_3$ powder was dissolved in a concentrated HCl + HNO_3 solution, followed by gentle heating for 10 min and dilution. A preliminary study was then made on the sinterability of these $BaTiO_3$ powders by pelleting them at a uniaxial pressure of 120 MPa and then at an isostatic pressure of 350 MPa, before being sintered for 2 h at 1250° and 1325°C, respectively. The sintered density was measured using the Archimedes method in distilled water, into which a few drops of wetting agent were added.

III. Results and Discussion

Figure 2(a) shows the partial phase diagram established at room temperature for the ternary system consisting of cyclohexane, NP5 + NP9, and an aqueous solution containing 0.12*M* $Ba(NO_3)_2$ + 0.12*M* $TiO(NO_3)_2$. Similarly, the partial phase diagram for the ternary system containing 0.34*M* $H_2C_2O_4$ as the aqueous phase is shown in Fig. 2(b). In both systems, the microemulsion region widens with increasing NP5 + NP9 to cyclohexane ratio, although the system containing 0.12*M* $Ba(NO_3)_2$ + 0.12*M* $TiO(NO_3)_2$ exhibits a wider microemulsion composition than that containing 0.34*M* $H_2C_2O_4$. The surfactant-rich compositions are highly viscous, which poses problems in obtaining a homogeneous mixture. In both ternary systems, the composition of 64.0 wt% cyclohexane, 16.0 wt% NP5 + NP9, and 20.0 wt% aqueous phase is within the microemulsion region.

Figure 3 shows the TGA and DTA traces at a heating rate of 10°C/min in air for precursors CCR, SMC, and DMC. When the conventionally coprecipitated precursor was heated from room temperature to 950°C, it exhibited three apparent falls in specimen weight over the temperature ranges from 50° to 120°C, 330° to 400°C, and 680° to 710°C, respectively. Each of these falls in specimen weight corresponds to an endothermic reaction on the DTA curve. It is generally accepted that the formation of barium titanate from barium titanium oxalate precursors involves the following three steps with increasing calcination temperature, although there are strong arguments for the types of intermediate phases involved:[30–32] (i) dehydration of the oxalate precursor, for example, the conversion of $BaTiO(C_2O_4)_2 \cdot 4H_2O$ to $BaTiO(C_2O_4)_2$; (ii) decomposition of $BaTiO(C_2O_4)_2$ to form intermediate phases, such as $BaCO_3$, TiO_2, $BaTi_2O_5$, and $Ba_2Ti_2O_5CO_3$; and (iii) formation of $BaTiO_3$ as a result of the reaction between the intermediate phases or the decomposition of the metastable $Ba_2Ti_2O_5CO_3$. The three falls in specimen weight are therefore believed to correspond to the above three stages, respectively. There is a close agreement between the overall weight loss of 47.7% observed when the precursor is heated to 950°C and that expected on the basis of the conversion from $BaTiO(C_2O_4)_2 \cdot 4H_2O$ to $BaTiO_3$ (46.8%).[5,18] To further support this, Fig. 4 shows the FTIR spectra for precursors CCR, SMC, and DMC calcined at various temperatures, respectively. The strong absorption band at around 1440 cm^{-1}, together with those at ~2450, 1752, 1060, and 859 cm^{-1}, detected in the conventionally coprecipitated powder calcined at 550°C indicates the presence of a carbonate phase.[7,33] These absorption bands decrease in intensity with increasing calcination temperature and most of them will almost completely disappear from the spectrum when the calcination temperature is raised to 800°C. As will be discussed later, XRD phase analyses show that the carbonate phase is crystalline $BaCO_3$, which is therefore believed to be one of the major phases involved in the conversion of barium titanium

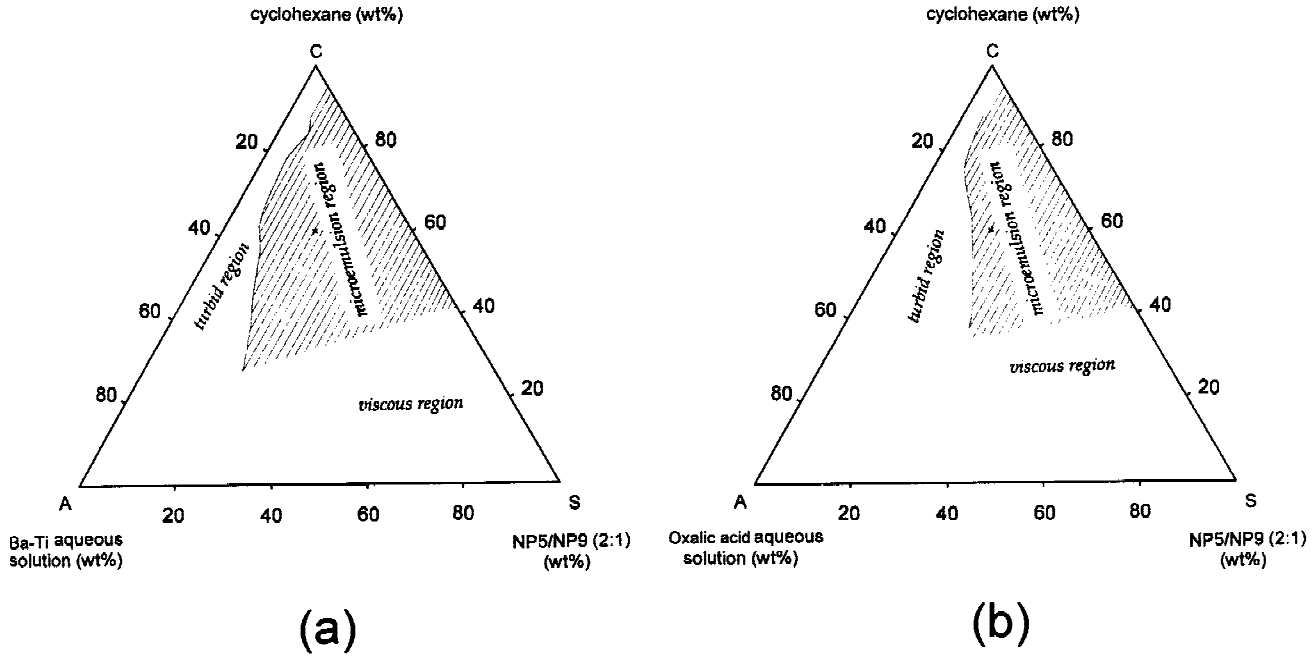

Fig. 2. Partial phase diagram established at room temperature for the ternary system consisting of cyclohexane, NP5 + NP9, and aqueous solution containing (a) 0.12*M* $Ba(NO_3)_2$ + 0.12*M* $TiO(NO_3)_2$ and (b) 0.34*M* oxalic acid.

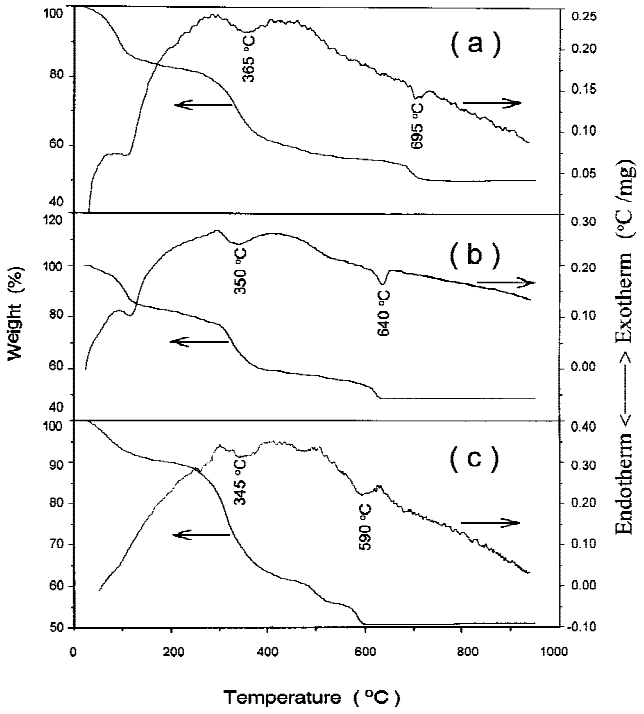

Fig. 3. TGA and DTA traces at a heating rate of 10°C/min in air for the precursors prepared via (a) the conventional coprecipitation reaction (CCR), (b) single-microemulsion coprecipitation using diether oxalate as the precipitant (SMC), and (c) double-microemulsion coprecipitation using oxalic acid as the precipitant (DMC).

oxalates to barium titanate with increasing calcination temperature. Most of the carbonate-related absorption bands were also observed in precursors SMC and DMC when they were calcined at low temperatures. As indicated in Fig. 4, however, both SMC and DMC exhibit a much weaker absorption band at around 1440 cm^{-1} than that for the conventionally coprecipitated powder when they are all calcined at 800°C for 2 h. It was estimated on the basis of these FTIR analyses that ~0.2 wt% $BaCO_3$ existed in the two-microemulsion-derived barium titanate powders. The impurity level was also indicated using a

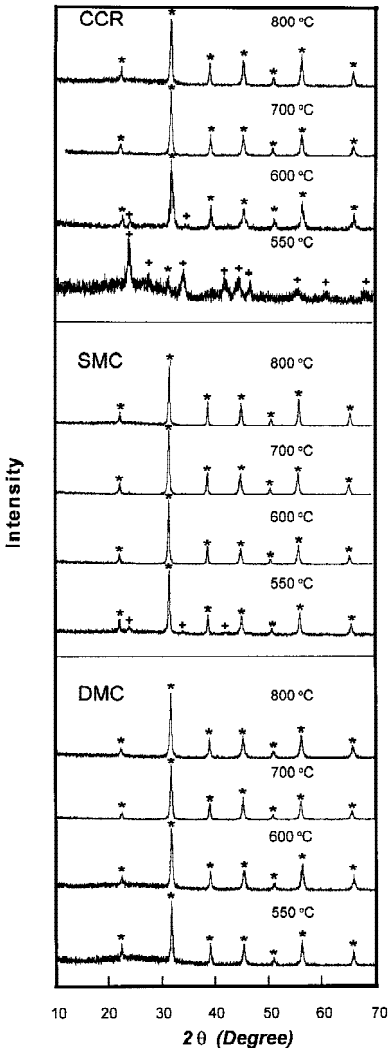

Fig. 5. XRD traces of the $BaTiO_3$ powders calcined for 2 h at various temperatures and prepared via the conventional coprecipitation reaction, and the single-microemulsion and double-microemulsion processing routes, respectively: (*) perovskite phase, (+) $BaCO_3$ phase.

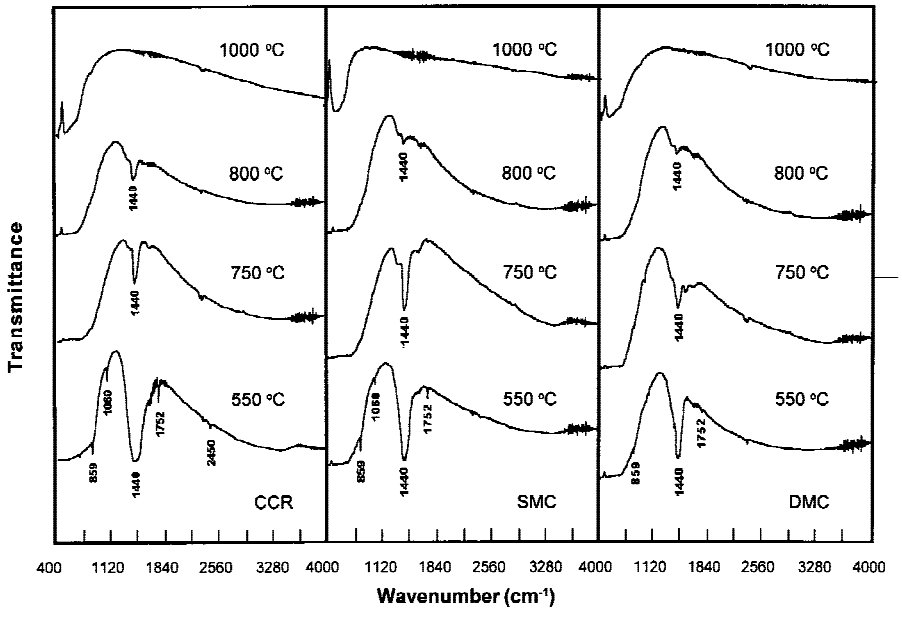

Fig. 4. FTIR spectra for the powders derived via the CCR, SMC, and DMC routes and calcined at various temperatures.

Perkin-Elmer elemental analyzer (2400 CHN) for carbon content in these powders.

Three steps in specimen weight, each corresponding to an endothermic reaction, are also observed in the precursor derived via the single-microemulsion route. The first two of the three occur over almost the same temperature ranges as those for the conventionally coprecipitated precursor. The remaining one, however, occurs at ~640°C, which is almost 55°C lower than that in the conventionally coprecipitated precursor. Similarly, the first two of the major falls in specimen weight observed for the precursor derived via the double-microemulsion route occur over temperature ranges similar to those for the conventionally coprecipitated precursor. This is followed by a two-step fall in specimen weight over the temperature range of 480° to 595°C. A minor and broadened exothermic peak correlates to the first step of the fall in specimen weight at around 505°C, presumably due to the oxidation of organic residuals. The final fall in specimen weight at around 590°C is associated with an endothermic peak observed on the DTA curve. It is apparent that the weight loss in precursor DMC is completed at ~595°C, which is below that observed for precursor SMC and is much lower than that of the conventionally coprecipitated precursor.

To study the phase development with increasing calcination temperature in each of the above three precursors, they were calcined in air to various temperatures in the range from 550° to 1000°C at a heating rate of 10°C/min, followed by phase and structure analyses using XRD and Raman spectrometer. Figure 5 shows the XRD patterns for precursors CCR, SMC, and DMC calcined at various temperatures over the range from 550° to 800°C, respectively. $BaCO_3$ was the predominant crystalline phase detected in the conventionally coprecipitated precursor calcined at 550°C, indicating that it was one of the major intermediate phases involved during the conversion of the oxalate precursor into $BaTiO_3$ with increasing calcination temperature. $BaTiO_3$ became the predominant phase when the precursor was calcined at 600°C. However, the carbonate phase was not completely eliminated until the calcination temperature was raised to 700°C. In contrast, a high-purity perovskite $BaTiO_3$ phase was obtained in the precursor derived via the single-microemulsion processing route at a calcination temperature of 600°C. A further reduction in the formation temperature of a single-phase perovskite $BaTiO_3$ powder was observed in the precursor derived via the double-microemulsion route (550°C for 2 h). These XRD phase analysis results show that the three precursors are considerably different in the calcination temperature required to develop a high-purity $BaTiO_3$ phase.

To further support the belief that the formation of $BaTiO_3$ in the two-microemulsion-derived oxalate precursors is completed at a lower temperature than that in the conventionally coprecipitated precursor (more specifically, the formation temperature follows DMC < SMC < CCR), the powder precursors calcined at various temperatures ranging from 700° to 1000°C were characterized using a Raman spectroscopy. Figure 6 shows the Raman spectra of powders CCR, SMC, and DMC calcined at 700°, 750°, 800°, and 1000°C. They all exhibit two distinct bands at ~310 and 720 cm^{-1}, indicating the presence of tetragonal phase. The very strong resemblance of these spectra

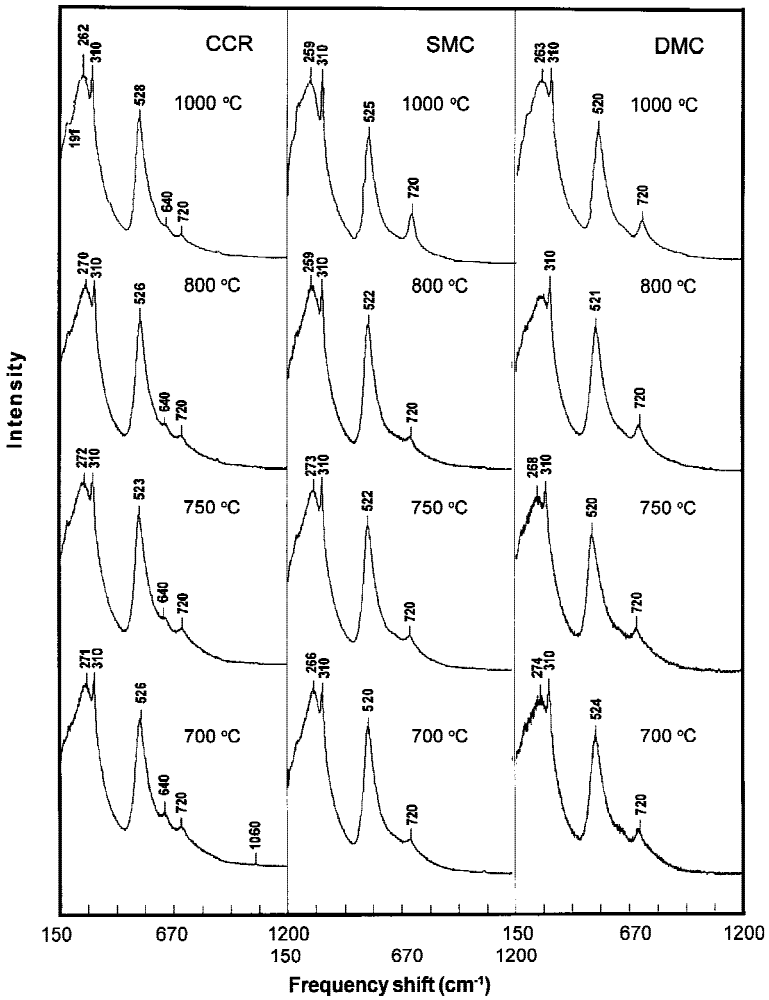

Fig. 6. Raman spectra of the $BaTiO_3$ powders derived via the conventional coprecipitation reaction, and the single-microemulsion and double-microemulsion processing routes, and calcined at 700°, 750°, 800°, and 1000°C for 2 h, respectively.

to that of a commercially available tetragonal barium titanate powder (99.9%, Johnson Matthey, USA) confirms that they are in the tetragonal form. Figure 6 also reveals two minor bands at ~640 and 1060 cm^{-1}, respectively, occurring in the conventionally coprecipitated barium titanate powder calcined at 700°C. They were not observed in the two-microemulsion-derived powders calcined at temperatures above 600°C. The 640 cm^{-1} band corresponds to the principal band of TiO_2, which, as an impurity phase in the conventionally coprecipitated barium titanate powder, cannot be eliminated by calcination at temperatures up to 1000°C. The 1060 cm^{-1} band is related to the carbonate, which was observed in the conventionally coprecipitated precursors calcined at temperatures below 700°C. This is consistent with the suggestion that the formation of $BaTiO_3$ involves $BaCO_3$ as an intermediate phase, which reacts with TiO_2 to form $BaTiO_3$.[30–32]

Table I. BET Specific Surface Area and Equivalent Discrete Particle Size of Various Calcined $BaTiO_3$ Powders

Temp (°C)	Specific surface area (m^2/g)			Equivalent discrete particle size (nm)		
	DMC	SMC	CCR	DMC	SMC	CCR
650	43.83	31.61	26.87	22.7	31.5	37.1
700	31.59	29.39	7.72	31.6	33.9	129.1
750	26.77	21.52	4.85	37.2	46.3	205.5
800	24.16	7.56	3.57	41.3	131.8	279.2

The $BaTiO_3$ powders derived via the above three processing routes are also different in crystallite and powder characteristics, such as the crystallite size, particle size, and particle morphology. Figure 7(a) plots the average crystallite size as a function of calcination temperature for powders CCR, SMC, and DMC. At each calcination temperature, the double-microemulsion-derived barium titanate powder exhibits the smallest crystallite size, followed by that derived via the single-microemulsion route. The conventionally coprecipitated barium titanate shows a much larger crystallite size than those of the other two. As expected, the crystallite size increases with increasing calcination temperature over the range from 550° to 800°C and with increasing calcination time at 750°C for all three powders, although the increase rate varies with calcination time as shown in Fig. 7(b).

Table I shows the specific surface area (BET) of calcined $BaTiO_3$ powders at various temperatures for 2 h, derived via the CCR, SMC, and DMC routes, respectively. The equivalent discrete particles sizes were worked out by assuming that they all consisted of monosized particles. The conventionally coprecipitated powder shows the lowest specific surface area

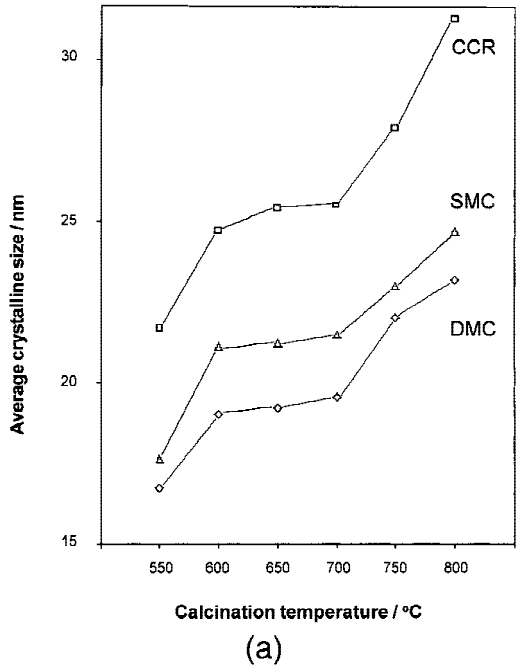

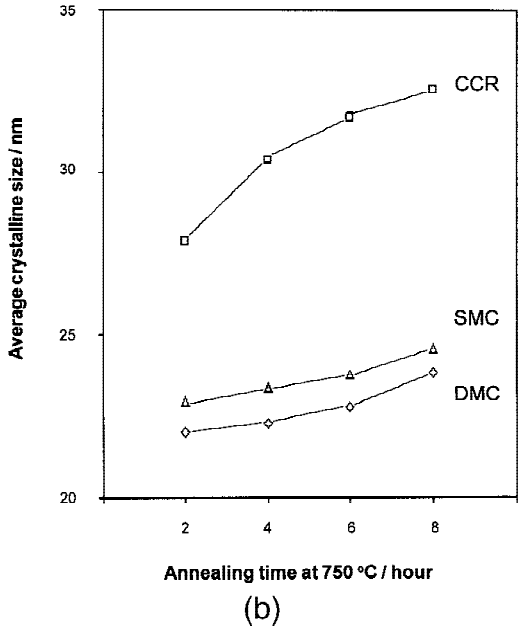

Fig. 7. (a) Average crystalline size estimated on the basis of peak (110) broadening as a function of temperature for the powders derived via the conventional coprecipitation reaction, and the single-microemulsion and double-microemulsion processing routes, respectively. (b) Average crystalline size estimated on the basis of peak (110) broadening as a function of annealing time at 750°C for the powders derived via the conventional coprecipitation reaction, and the single-microemulsion and double-microemulsion processing routes, respectively.

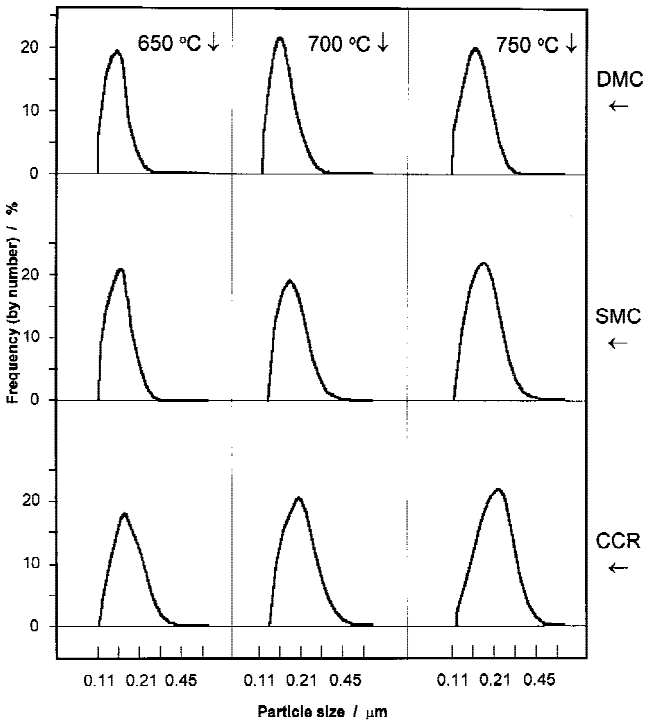

Fig. 8. Particle/aggromerate size distribution of $BaTiO_3$ powders derived via the conventional coprecipitation reaction, the single-microemulsion and double-microemulsion processing routes, and calcined at 650°, 700°, and 750°C, respectively.

among the three at each calcination temperature and furthermore it demonstrates a dramatic fall in specific surface area when the calcination temperatures is raised from 650° to 700°C. In contrast, the double-microemulsion-derived powder exhibits the highest specific surface area and therefore the smallest discrete particle size at each calcination temperature, followed by the single-microemulsion-derived powder. This demonstrates the effectiveness of microemulsion processing in obtaining an ultrafine $BaTiO_3$ powder.

As shown in Fig. 8, the two-microemulsion-derived barium titanate powders were also smaller in average particle/agglomerate size than that of the conventionally coprecipitated powder, as measured using light scattering technique. To reduce the effect of particle agglomeration on the measured particle size distributions, each powder was dispersed in deionized water and ultrasonically stirred for 20 min before a test was carried out. It is apparent that the average particle/agglomerate size follows the order of CCR > SMC > DMC at each calcination temperature. To further demonstrate the particle/agglomerate size distribution and particle morphology, Figs. 9(a–c) and 10(a–c) are SEM micrographs showing the microstructure of the three barium titanate powders calcined at 650° and 800°C, respectively. Particle agglomerates of 5 to 10 μm in sizes dominate the conventionally coprecipitated powder,

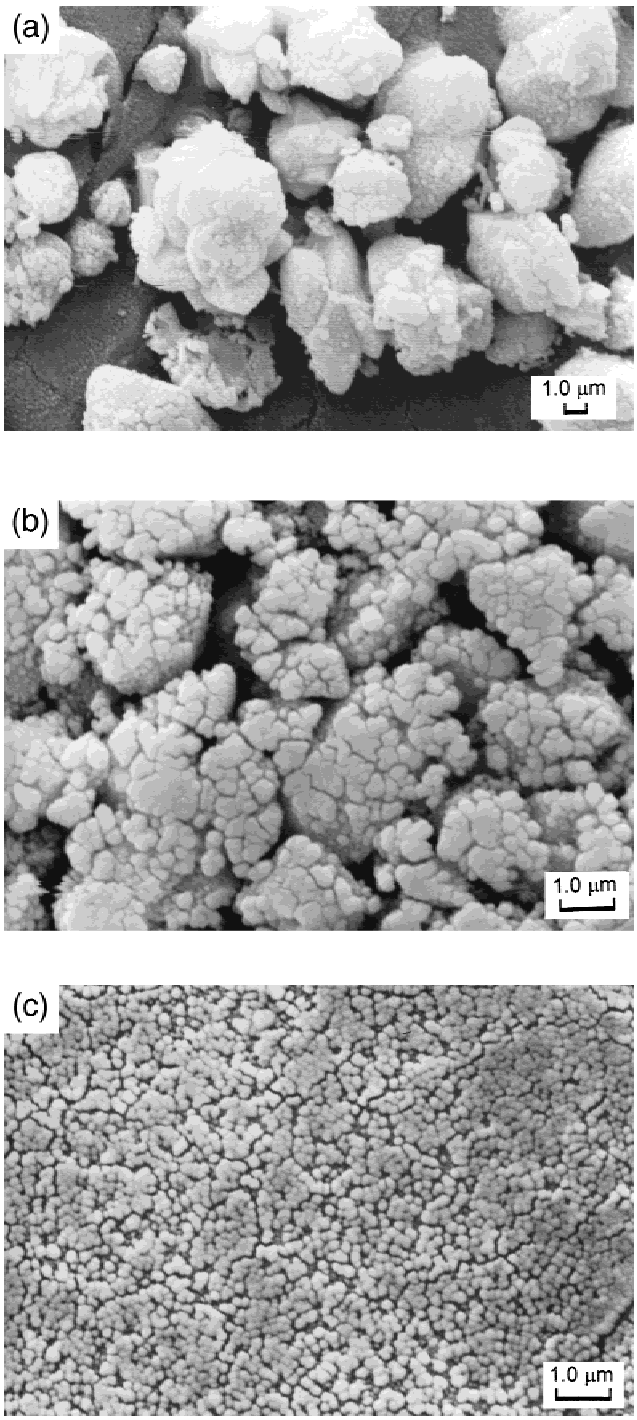

Fig. 9. Three SEM micrographs showing the powders calcined at 650°C for 2 h, derived via (a) the conventional coprecipitation reaction, (b) the single-microemulsion and (c) double-microemulsion processing routes, respectively.

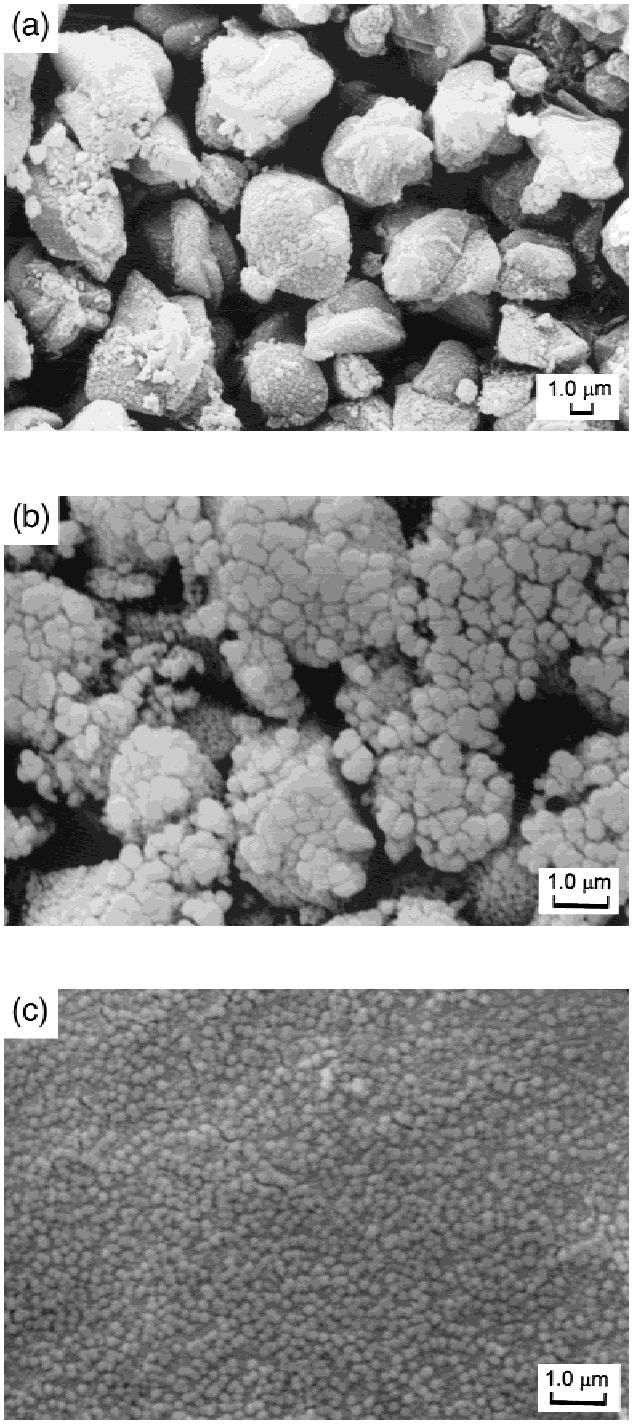

Fig. 10. Three SEM micrographs showing the powders calcined at 800°C for 2 h, derived via (a) the conventional coprecipitation reaction, (b) the single-microemulsion and (c) double-microemulsion processing routes, respectively.

although discrete particles are much smaller. The single-microemulsion-derived powder consists of loosely packed particle agglomerates 3 to 5 μm in size. In a remarkable contrast, the double-microemulsion-derived barium titanate powder consists of well-dispersed spherical barium titanate particles ~100 nm in diameter, which are almost agglomerate-free. Figures 11(a–c) are three TEM micrographs further showing the differences among the three barium titanate powders calcined at 800°C in crystallite size, particle morphology, and the degree of particle agglomeration.

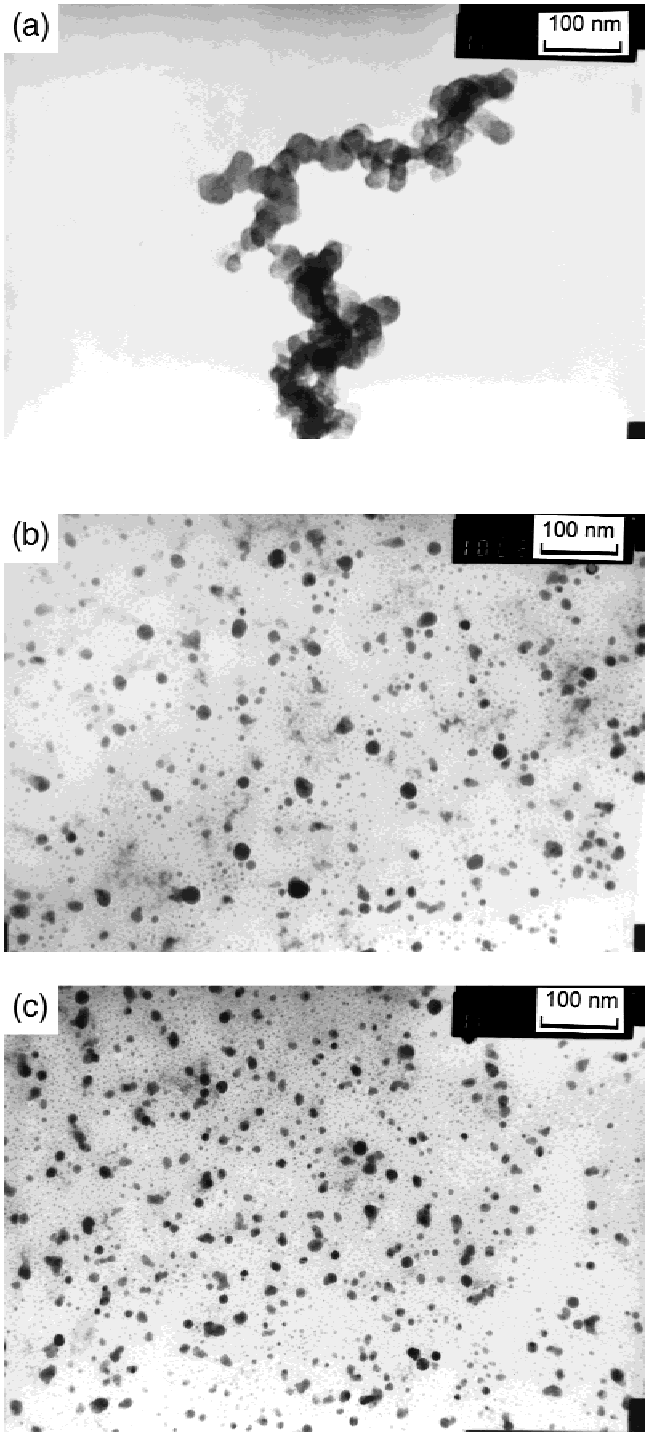

Fig. 11. Three TEM micrographs showing the powders calcined at 800°C for 2 h, derived via (a) the conventional coprecipitation reaction, and (b) the single-microemulsion and (c) double-microemulsion processing routes, respectively. The TEM samples were prepared by mechanically dispersing the powders in ethanol.

As expected on the basis of the refinement in particle characteristics, the two-microemulsion-derived barium titanate powders exhibit better sintering behavior than that of the conventionally coprecipitated one. For example, the former two were sintered to ~96% theoretical density at 1250°C for 2 h, compared to ~92% for the latter at the same temperature. A sintered density of >99% theoretical was obtained for the two-microemulsion-derived barium titanates at 1325°C for 2 h, in contrast to <96% for the conventionally coprecipitated barium titanate at the same temperature. One of the concerns in employing microemulsions for synthesizing barium titanate is the Ba/Ti ratio in the resulting powders. As in many other wet chemical routes, there is a possibility of losing more barium than titanium because of their difference in solubility. However, the degree of Ba deficiency in the two-microemulsion-derived barium titanate powders prepared in this work is minimal, as supported by a Ba/Ti ratio of ~0.996 worked out for them using ICP.

IV. Conclusions

Barium titanate powders were prepared via three chemical-based processing routes, namely, conventional coprecipitation, single-microemulsion coprecipitation using diether oxalate as the precipitant, and double-microemulsion coprecipitation using oxalic acid as the precipitant. A single-phase perovskite barium titanate was obtained when the double-microemulsion-derived oxalate precursor was calcined for 2 h at 550°C, compared to 600°C required by the single-microemulsion-derived precursor. A calcination at >700°C for 2 h was required for the conventionally coprecipitated precursor in order to develop a predominant barium titanate phase. It was, however, impossible to eliminate the residual TiO_2 phase in the coprecipitated $BaTiO_3$ powder by raising calcination temperature up to 1000°C. All three barium titanate powders exhibited a tetragonal structure when calcined at 700°C and above. The microemulsion-derived barium titanate powders also demonstrated much better powder characteristics, such as more refined crystallite and particle sizes and a much lower degree of particle agglomeration, than those of the conventionally coprecipitated powder.

Acknowledgment: We wish to acknowledge Miss Chai Hoon Quek for her technical assistance with the TEM images.

References

[1]P. P. Phule, and S. H. Risbud, "Review: Low-Temperature Synthesis and Processing of Electronic Materials in the BaO–TiO_2 System," *J. Mater. Sci.*, **25**, 1169–83 (1990).

[2]A. D. Hilton and R. Frost, "Recent Developments in the Manufacture of Barium Titanate Powders," *Key Eng. Mater.*, **66–67**, 145–84 (1992).

[3]A. Beauger, J. C. Mutin, and J. C. Niepce, "Synthesis Reaction of Metatitanate $BaTiO_3$—Part 2, Study of Solid–Solid Interfaces," *J. Mater. Sci.*, **18**, 3543–50 (1983).

[4]S. Kim, M. Lee, T. Noh, and C. Lee, "Preparation of Barium Titanate by Homogeneous Precipitation," *J. Mater. Sci.*, **31**, 3643–45 (1996).

[5]T. Tunkasiri and G. Rujijanagul, "Characterization of Barium Titanate Prepared by Precipitation Technique," *J. Mater. Sci. Lett.*, **13**, 165–69 (1994).

[6]T.-T. Fang, H.-B. Lin, and J.-B. Hwang, "Thermal Analysis of Precursors of Barium Titanate Prepared by Coprecipitation," *J. Am. Ceram. Soc.*, **73**, 3363–67 (1990).

[7]M. H. Frey and D. A. Payne, "Synthesis and Processing of Barium Titanate Ceramics from Alkoxide Solutions and Monolithic Gels," *Chem. Mater.*, **7**, 123–29 (1995).

[8]C. Lemoine, B. Gilbert, B. Michaux, J.-P. Pirard, and A. Lecloux, "Synthesis of Barium Titanate by the Sol–Gel Process," *J. Non-Cryst. Solids*, **175**, 1–13 (1994).

[9]P. P. Phule and S. H. Risbud, "Sol–Gel Synthesis of Barium Titanate Powder Using Barium Acetate and Titanium(IV) Isopropoxide," *Adv. Ceram. Mater.*, **3**, 183–85 (1988).

[10]P. K. Dutta, R. Asiaie, S. A. Akbar, and W. Zhu, "Hydrothermal Synthesis and Dielectric Properties of Tetragonal $BaTiO_3$," *Chem. Mater.*, 6, 1542–48 (1994).

[11]K. Fukai, K. Hikada, M. Aoki, and K. Abe, "Preparation and Properties of Uniform Fine Perovskite Powders by Hydrothermal Synthesis," *Ceram. Int.*, **16**, 285–90 (1990).

[12]Y. Ito, S. Shimada, and M. Inagaki, "Molten-Salt Synthesis of

$Ba_{1-x}Pb_xTiO_3$ in the System $BaTiO_3$–$PbCl_2$," *J. Am. Ceram. Soc.*, **78**, 2695–99 (1995).

[13]Y. Ito, S. Shimada, J. Takahashi, and M. Inagaki, "Phase Transition of $BaTiO_3$–$Ba_{1-x}Pb_xTiO_3$ Composite Particles Prepared by the Molten Salt Method," *J. Mater. Chem.*, **7**, 781–85 (1997).

[14]M. Arima, M. Kakihana, Y. Nakamura, M. Yashima, and M. Yoshimura, "Polymerized Complex Route to Barium Titanate Powders Using Barium–Titanium Mixed-Metal Citric Acid Complex," *J. Am. Ceram. Soc.*, **79**, 2847–56 (1996).

[15]N. G. Eror and H. U. Anderson, "Polymeric Precursor Synthesis of Ceramic Materials," *Mater. Res. Soc. Symp. Proc.*, **73**, 571–78 (1986).

[16]M. Stockenhuber, H. Mayer, and J. A. Lercher, "Preparation of Barium Titanates from Oxalates," *J. Am. Ceram. Soc.*, **76**, 1185–90 (1993).

[17]H. S. Potdar, P. Singh, S. B. Deshpande, P. D. Godbole, and S. K. Date, "Low-Temperature Synthesis of Ultrafine Barium Titanate ($BaTiO_3$) Using Organometallic Barium and Titanium Precursors," *Mater. Lett.*, **10**, 112–17 (1990).

[18]H. Yamamura, A. Watanabe, S. Shirasaki, Y. Moriyoshi, and M. Tanada, "Preparation of Barium Titanate by Oxalate Method in Ethanol Solution," *Ceram. Int.*, **11**, 17–22 (1985).

[19]C. Miot, C. Proustz, E. Husson, R. Erre, G. Blondiaux, J. M. Beny, and J. P. Coutures, "Characterization of Barium Titanate Ceramics Obtained by a Chemical Route after Laser Ablation," *Mater. Sci. Eng.*, **B45**, 17–24 (1997).

[20]J. P. Coutures, P. Odier, and C. Proust, "Barium Titanate Formation by Organic Resins Formed with Mixed Citrate," *J. Mater. Sci.*, **27**, 1849–56 (1992).

[21]G. A. Hutchins, G. H. Maher, and S. D. Ross, "Control of the Ba:Ti Ratio of $BaTiO_3$ at a Value of Exactly 1 via Conversion to $BaO{\cdot}TiO_2{\cdot}3C_6H_8O_7{\cdot}3H_2O$," *Am. Ceram. Soc. Bull.*, **66**, 681–84 (1987).

[22]F. Chaput, J. P. Boilot, and A. Beauger, "Alkoxide–Hydroxide Route to Synthetize $BaTiO_3$-Based Powders," *J. Am. Ceram. Soc.*, **73**, 942–48 (1990).

[23]J. Fang, J. Wang, S.-C. Ng, C.-H. Chew, and L.-M. Gan, "Ultrafine Zirconia Powders via Microemulsion Processing Route," *Nanostruct. Mater.*, **8**, 499–505 (1997).

[24]L. M. Gan, L. H. Zhang, H. S. O. Chan, C. H. Chew, and B. H. Loo, "A Novel Method for the Synthesis of Perovskite-Type Mixed Metal Oxides by the Inverse Microemulsion Technique," *J. Mater. Sci.*, **31**, 1071–79 (1996).

[25]H. Herrig and R. Hempelmann, "A Colloidal Approach to Nanometre-Sized Mixed Oxide Ceramic Powders," *Mater. Lett.*, **27**, 287–92 (1996).

[26]S. E. Friberg and P. Bothorel, *Microemulsions: Structure and Dynamics.* CRC, Boca Raton, FL, 1986.

[27]S. Schlag, H.-F. Eicke, D. Mathys, and R. Guggenheim, "Preparation of Submicrometer Ferroelectric Particles by Wet-Chemical Methods," *Langmuir*, **10**, 3357–61 (1994).

[28]K. Kudaka, K. Ilzumi, and K. Sasaki, "Preparation of Stoichiometric Barium Titanyl Oxalate Tetrahydrate," *Am. Ceram. Soc. Bull.*, **61**, 1236–36 (1982).

[29]H. P. Klug and L. E. Alexander, "X-ray Diffraction Procedures for Polycrystalline and Amorphous Materials"; pp. 491–538 in *Crystallite-Size Determination from Line Broadening.* Wiley, New York, 1954.

[30]M. Stockenhuber, H. Mayer, and J. A. Lercher, "Preparation of Barium Titanates from Oxalate," *J. Am. Ceram. Soc.*, **76**, 1185–90 (1993).

[31]P. K. Gallagher and J. Thomson, Jr., "Thermal Analysis of Some Barium and Strontium Titanyl Oxalates," *J. Am. Ceram. Soc.*, **48**, 644–47 (1965).

[32]S. Kumar, G. L. Messing, and W. B. White, "Metal Organic Resin Derived Barium Titanate: I, Formation of Barium Titanium Oxycarbonate Intermediate," *J. Am. Ceram. Soc.*, **76**, 617–24 (1993).

[33]R. A. Nyquist and R. O. Kagel, *The Handbook of Infrared and Raman Spectra of Inorganic Compounds and Organic Salts, Vol. 4, Infrared Spectra of Inorganic Compounds*; pp. 78–79. Academic Press, New York, 1997. □